

A visco-elastoplastic constitutive model for large deformation response of polycarbonate over a wide range of strain rates and temperatures

Peng Yu ^a, Xiaohu Yao ^{a,*}, Qiang Han ^a, Shuguang Zang ^b, Yabei Gu ^c

^a South China University of Technology, Guangzhou 510640, China

^b China Building Material Test and Certification Center, Beijing 100024, China

^c PPG Industries, Inc., Glass Business and Discovery Center, Pittsburgh 15024, USA



ARTICLE INFO

Article history:

Received 27 June 2014

Received in revised form

3 September 2014

Accepted 28 September 2014

Available online 22 October 2014

Keywords:

Rate-thermomechanical

Visco-elastoplastic

Constitutive model

ABSTRACT

The principal purpose in this paper is to present a combined experimental and analytical study to understand the mechanical behavior of polycarbonate (PC) under a wide range of temperatures (-40°C to 100°C) and strain rates (0.001 up to 5000 s^{-1}). Firstly, the experiments were conducted to obtain stress-strain response from low to high rates and temperatures. Then a robust physically consistent rate and temperature-dependent constitutive model is proposed to characterize large deformation mechanical behavior of PC. According to viscoelastic theory, a nonlinear-viscoelastic model is employed to understand the elastic response. Yielding behavior is described via cooperative model. As respect to post-yield regime, it is described by the conflict and interaction between softening and hardening behavior based on the integral-form softening and kinematic hardening model. The proposed constitutive model is successfully validated by the excellent agreement between model prediction and experiment results.

© 2014 Elsevier Ltd. All rights reserved.

1. Introduction

Polycarbonate (PC) is one of the most characterized polymers in the documented research. Due to the transparent property and good performance in impact resistance, it is widely applied as structural components in engineering fields, ranging from windshields of aircraft and vehicle, helmets, body armors to bulletproof glasses of bank. As temperatures and strain rates often have a great influence on PC, it is essential to develop a rate and temperature-dependent constitutive model to capture its mechanical behaviors.

Numerous studies have been made to elucidate the mechanical response of polymer glass worldwide. Most current existing constitutive models derive from original work of Haward and Thackray [1]. They employed two paralleling model, combined with Eyring [2] viscosity, to describe elastic and post-yield for polymer material. This original 1D model, restricted to a linear elastic response up to yield was later improved and extended by 3 main research groups: groups of Mary Boyce in MIT [3–5], groups of Paul Buckley in Oxford [6–8], and groups of Govaert in Eindhoven [9–11]. They introduced strain softening, strain hardening as well

as pressure dependence [3,6,12–16] to improve the model. All of their efforts were later summarized to the well-known BPA (groups of Mary Boyce in MIT), OGR (groups of Paul Buckley in Oxford), EGP (groups of Govaert in Eindhoven) model. These three models have made contributions to constitutive model of glassy polymer from different degrees, involving elasticity, yielding, softening, hardening and unloading phase. Based on the Ree-Eyring theory and modification of the general Eyring theory [5,17] which explained the transition observed in the yield behavior in terms of molecular-level motions, and connecting molecular mechanisms of deformation resistance with macroscopic mechanical behavior which was furthered by Bauwens [18], Boyce et al. [19] improved the model by using primary (α) process where intermolecular resistance is generated in the elastic spring and viscoplastic dashpot at high temperatures and low strain, in parallel with the most significant secondary process (β) which is fairly compliant, most at high temperatures and low strain rates and restricted at low temperatures and high strain rates. Upon this basis, Safari et al. [20] added another secondary rate-activated processes (γ) to capture deformation of polycarbonate during high strain rate. For presenting the stress in the non-linear hardening, a non-linear Lan-gevin spring was applied to characterize ‘back stress’ network, which results from the entropic resistance to molecular alignment. BPA model was later modified [21] by taking account of the current

* Corresponding author. Tel./fax: +86 020 87114460.

E-mail address: yaoxh@scut.edu.cn (X. Yao).

temperature and the current effective strain rate for elastic modulus and introducing two internal variables to display strain softening. The demonstration of post-yield behavior of polymer glass was perfect, especially connecting to molecular mechanisms. However, little attention has been paid to pre-yield behavior, particularly viscous contributions, or more definitely, elasticity is just regarded as a transition process in BPA model. As to the OGR model, incorporating reduction of Vogel temperature arisen from chain ends in multimode form, Buckley et al. [6] predicted closely both linear viscoelastic response, plastic flow and a fall in yield stress with reducing molecular length. Afterward, the degree of strain-hardening in the model was observed by De Focatiis et al. [7] to increase along with increasing prior stretch of molecules within the entanglement tubes. The OGR model captured the features of both melt and glassy state of polymer glasses. Compared with BPA and OGR model, a ‘compressible-Leonov model’ was proposed by Tervoort et al. [11] to separate the visco-elastic volume response from the elasto-viscoplastic isochoric deformation. By this way, a spectrum of relaxation times can be involved and determined in visco-elastic model directly. This was the early EGP model and later furthered by Govaert et al. [9], who connected homogeneous plastic deformation behavior observed in PC samples with numerical analysis of the ‘mechanical rejuvenation’ and intrinsic strain softening to cover phenomenological aspects of the large strain mechanical behavior of glassy polymers. Recently, an optimized EGP constitutive model with multiple relaxation times for polymer glasses has been elaborated by van Breemen et al. [22]. This multimode, consisting of the relaxation time spectrum obtained from a simple series of tensile experiments, predict quantitatively the intrinsic polymer response of PC, especially the non-linear visco-elastic and unloading region. However, the question is that, in order to obtain proper agreement with experiment results for PC, massive modes parameters are required to be quantified, which will lead to a troublesome work.

There are also other documented contributions to constitutive model for polymer materials. Elastic–viscoplastic constitutive models based on overstress derived from the unified state variable theory for metallic materials were applied to polymers by Khan et al. [23] and Colak et al. [24]. Ghorbel et al. [25] employed the general principles of thermo-dynamics with internal variables for standard generalized materials to represent the mechanical behavior of polymeric materials. Senden et al. [26] used a part of the rubber-elastic to replace the viscous contribution to capture both the strain rate and temperature dependence of strain hardening of PC. Bouvard et al. [27] applied a hierarchical multi-scale approach for bridging mechanisms from the molecular scale to the continuum scale to select the internal state variables and developed a temperature dependence and time-dependent material model for amorphous PC. In addition, it is necessary to mention the robust work done by Richeton et al. [28–33] for the mechanical behavior of polymers. They proposed a unified model for prediction of the stiffness modulus with the influence by frequencies/strain rates and temperatures to describe the elastic property of polymers [33]. Also, they built a formulation of cooperative model based on superposition principle to capture the yield behavior of amorphous polymers for a wide range of strain rates and temperatures [31]. As to the post-yield stage, a hardening model, wherein the intra-molecular and intermolecular interaction are considered, was established by Richeton et al. [32] to characterize the mechanism of plastic deformation of polymeric materials. Zhu et al. [34] constructed a constitutive model where the glassy resin matrix post-yield softening and progressive hardening behaviors were taken into consideration in multi-fiber composites. Their researches are so robust and physically consistent that it will make a lot of contributions to the work in this paper.

The primary objective of this paper is to propose a macroscopic phenomenological constitutive model, which is robust and physically based to understand the viscoelastic and viscoplastic large deformation response of PC over a wide range of rates and temperatures, covering the observable mechanical behavior including viscoelasticity, yielding, subsequent strain-softening and strain-hardening. Firstly, quasi-static and dynamic uniaxial compression experiment of PC, carried out by using a servohydraulic test machine and an iron split-Hopkinson pressure bar (SHPB), are presented. Then, based upon model of stiffness modulus proposed by Richeton et al. [33], a developed viscoelastic model is established to describe elastic response. Through the cooperative model, the temperature and strain rate dependence for yielding behavior can be well understood. After that, a model that incorporates conflict and interaction between the softening and hardening behavior is developed to catch the mechanical characteristics at the post-yielding phase. The proposed model focuses on explanation for features of PC from macroscopic and phenomenological aspect. It is acknowledged that a well-developed visco-elastoplastic constitutive model that can well catch the mechanical behavior of polymer materials is supposed to be quantitatively predictive for most experimental stress-strain curves to engineering accuracy using one set of material parameters. For this reason, significant parameters in model are considered as function of strain rate and temperature. Although this consideration would lead to more material constants, the parameters are almost determined directly from experimental results instead of extreme dependence on curve fitting, which distinguishes our work from previous efforts and also obliges us to validate it under an equally wide range of experimental conditions to assess its accuracy. Predictions from the proposed constitutive model exhibit good agreement with experimental data varying from low to high rates and temperatures.

2. Experiment

2.1. Materials and specimens preparation

The material used in this study is polycarbonate, provided by Bayer Company under brand name of Makrolon. All the samples were machined directly from sheet stock by China Building Material Test and Certification Center and stored in room temperature for 3–5 days before testing to eliminate any variability in the data caused by changing humidity levels.

2.2. Uniaxial compression test

Uniaxial compressions were carried out on PC over six decades of strain rate from 10^{-3} to 5000 s^{-1} over a wide range temperatures (from -40°C up to 100°C). Low rates (10^{-3} to 10^{-1} s^{-1}) testing was carried out on the servo-hydraulic machine. The samples for quasi-static test were of right circular cylinder geometry with diameter of 12 mm and length of 6 mm. This particular length-to-diameter ratio (1:2) was chosen to be consistent with the geometry of the high-rate specimens. Both up and down surface of the specimens were required to be polished before they were placed on test machine. Note that the dimensions of diameter and length were measured after polishing and parallel-face tolerance of each PC sample was less than 0.25%. Lubricant was applied between the loading plates and the specimen to avoid barreling and shearing phenomena.

High rate test (2000 – 5000 s^{-1}) was presented on compressive split-Hopkinson bar (SHPB) apparatus. The appliance consists of solid steel bars, involving incident and transmission bars with a length of 400 mm and a diameter of 14 mm as well as striker bar with 200 mm length and 14 mm diameter, the schematic description seen in Fig. 1. There have been a large number of

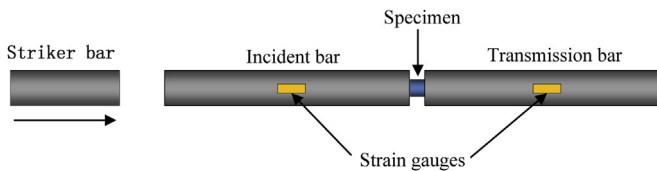


Fig. 1. The schematic representation of the SHPB.

investigations on principle of split-Hopkinson bar testing [35–39]. Among them, one of the most critical documented suggestions is that 1:2 ratio of length to diameter is essential for low impedance materials (such as PC in this study) on these test systems. To meet the requirement, the PC samples for SHPB were also designed to be right circular cylinder geometry, however, with a diameter of 6 mm and a length of 3 mm, much less than dimension of those conducted on servo-hydraulic machine. On the one hand, the less length enables the PC specimen achieve higher strain rate and dynamic equilibrium more readily based on the theory of stress wave [35]. On the other hand, the discrepancy of diameter between the specimen and bar contributes to decrease negative effect caused by wave impedance [35]. According to the research by Trautmann et al. [40], petroleum jelly is very suitable to be a good lubricant for PC in SHPB test at ambient (26°C) and low temperature (-60°C), because it is helpful to provide perfect lubrication to reduce friction to zero within experimental error during the test. As a result, petroleum jelly, as the lubrication was coated on both surface of specimen to limit the influence of barreling and shearing phenomena.

3. Results and analysis

The representative compression testing results on the servo-hydraulic instrument and SHPB are performed at in Fig. 1. The results are at low rates (0.001 s^{-1} to 0.1 s^{-1}) and over a wide range of temperature from -40°C to 100°C . At least 3 samples were tested in quasi-static experiment at each rate and temperature to make sure the data valid. Due to the limitation of the experimental conditions that we do not have the liquid nitrogen facility used for SHPB experiment, the experimental results in high rates at low temperatures were not obtained. But we are developing our experiment device and the relevant data will be got in the near future. The Fig. 2 shows the representative original wave shape for PC in the SHPB experiment at high strain rate in room temperature.

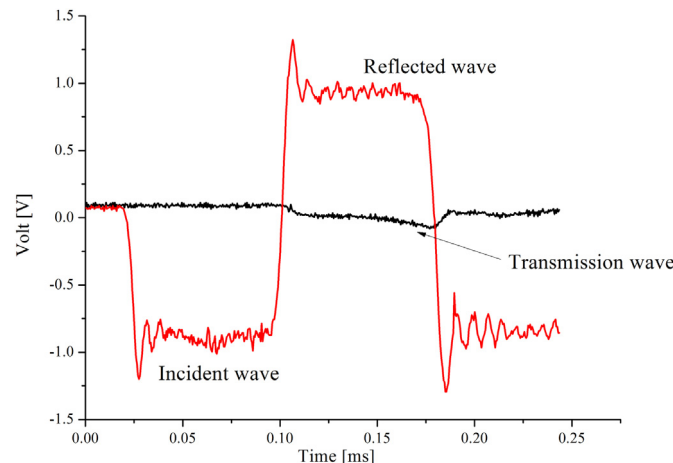


Fig. 2. The representative original signal for PC in SHPB experiment at high rate in room temperature.

After the filtering and measurement on the wave data, the plots between the true stress and strain rate versus true strain have been obtained in Fig. 3. Seen from the Fig. 3, when the sample stays at elastic phase, the strain rate increases with the larger deformation. As the PC goes into the plastic phase, the trend of the strain rate plot gradually reaches stably at about 5000 s^{-1} in the Fig. 3, which demonstrates the specimen gets to the dynamic equilibrium during the experiments. The true stress-strain curves generally occur ringing at high rate due to the dynamic loads by steel bar, so in order to get the clean experiment data in Fig. 6, at least 5 samples are firstly tested at the approximate high rate and then make the results averaged. Afterward, smooth the data with the bound less than 5% to get clean data, which is helpful to determine the material parameters in constitutive model without damaging the accuracy of the experimental results. This work is similar to that by Boyce [19]. Similar SHPB experiments have been conducted by Siviour et al. [41], Li et al. [42] and Lerch et al. [43]. Li and Lerch carried out temperature measurements on PC material during the tests by using a fast response infrared optical pyrometer and a high speed infrared HgCdTe detector array, respectively, which are able to monitor temperature change of the specimen. The range of PC strain rate in the experiment by Li and Lerch was varying from low rates up to about 2000 s^{-1} since the samples are much thicker (the thickness is 8 mm in Li's work) than those in this paper. In contrast, thickness of PC specimens in Siviour's work, which is 1.5 mm and 0.75 mm, is so much thinner that the rate of sample is easy to get high level in test. The comparison of PC SHPB experimental results between Li and Siviour is displayed in Fig. 4. It is clear that PC material performs dependence on strain rate in Li's work and on temperature in Siviour's work. As referred before, the thinner thickness in Siviour's work enables the PC arrives at higher strain rate and more easily reaches dynamic equilibrium simultaneously. That is why the plots in Siviour's work show less ringing than those in Li's work. Regardless of that, the plots in Fig. 4 well describe the mechanical behavior of the PC, as the experimental results in Fig. 6 in this article.

Seen from Figs. 3–5, the experimental outcomes illustrate common phenomenological mechanical response of PC observed in compression experiment. Regardless of low and high rates and temperatures, the PC specimens experience elastic phase firstly, and then reach the yield point. After that PC performs strain-softening behavior and subsequent strain-hardening behavior. At low strain rates, PC could deform even up to a true strain value 1.0, displaying a pretty good ductile character. While the strain of PC

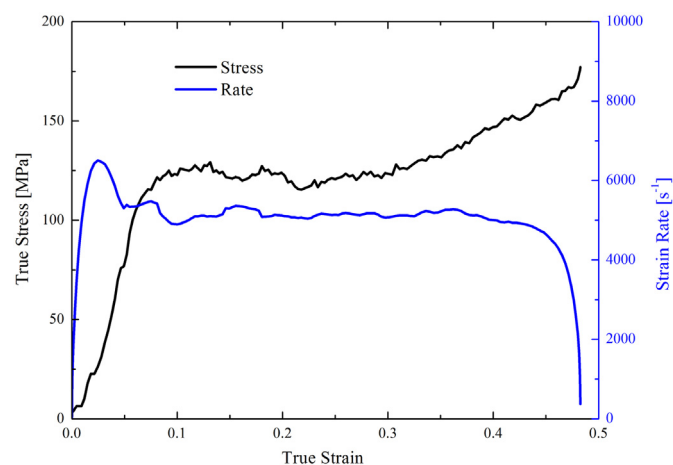


Fig. 3. The plots of true stress and strain rate versus true strain rate PC at about 5000 s^{-1} in room temperature.

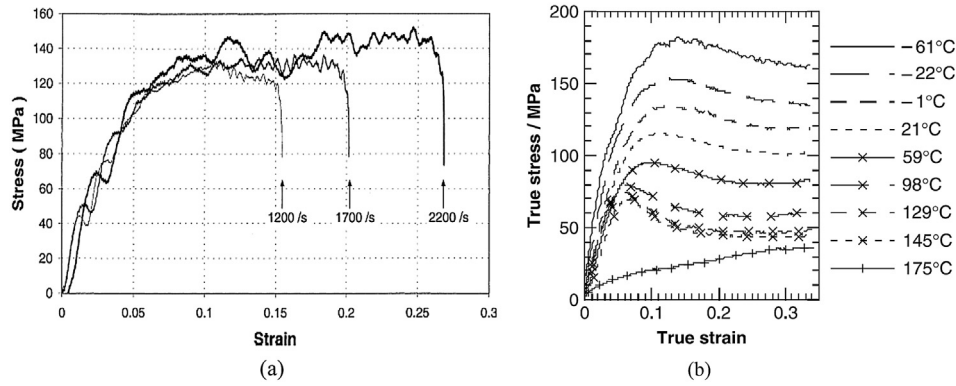


Fig. 4. The comparison of the PC material stress–strain curves in SHPB between Li [42] (a) and Sivouri [41] ((b), strain rate is $5500 \pm 500 \text{ s}^{-1}$).

samples increases with the growth of strain rates at high rates. That is because the high rates mean high impact speed of striker bar in SHPB test, in which more kinetic energy would lead to large deformation for PC. It should be pointed out that, unlike servo-hydraulic experiments where the strain rate of PC could be constant by controlling the loading speed constantly, in SHPB test, the strain rate of PC would go up and down until it reaches the dynamic equilibrium. As a result, the high strain rate labeled in Figs. 6,7 is average strain rate of relevant curve over duration of tests.

In addition, based on the compression experiment results, the mechanical responses of PC show great dependence on strain rates and temperatures. To be specific, despite of low and high rates, as strain rate increases, elastic modulus and yield stress go up, while as temperature increases, they both go down. Also, the behaviors of softening and hardening are temperature and rate-dependent. When the temperature rises, softening behavior are more easily to be observed. The evidence is that it performs much more apparently at high temperature than that at low temperature (seen in Fig. 5). Particularly, softening behavior of PC almost cannot be found very clearly at -40°C . That is because at low temperature, PC generally presents hardening resistance behavior. Therefore, as the temperature becomes lower, hardening behavior develops more quickly and extensively. In contrast, the increase of strain rate leads to the so-called weakness for softening behavior and the enhancement for hardening behavior. Something interesting can be found that sensitivity of the mechanical characters of PC within low rate regime behavior is comparable to that in high temperature.

This case can be explicitly explained by the well-known time temperature equivalence principle. Furthermore, in essence, the post-yielding regime is the interaction, more exactly, the conflict between the strain softening and strain hardening. At high temperatures and low rates, extent and of softening go so notably that PC often exhibits a large and deep slope of stress decrease at these states, which means the softening behavior is predominant compared to hardening. Conversely, when temperatures are low and strain rates are high, the observation is that the softening process nearly disappears and PC materials reach straightly the hardening phase that the stress increase dramatically as the deformation becomes larger. Overall, PC, as one of the most typical kinds of glassy polymer materials, generally experiences softening procedure at first after the yield, in other words, softening response often occupies a dominant position at the early stage of post-yield. While with the growth of the plastic deformation, the mechanical behavior of PC almost comes to hardening, that is to say, the hardening behavior will always beat the softening finally. It is due to the fact that as plastic deformation becomes larger, the molecular motion and mobility in microstructure will make the molecular chains stiffer, which often contributes to resistance between adjacent molecular segments and as a consequence these sharply strengthened resistant forces would cause the rapid rise for stress of PC samples in experiments.

4. Constitutive model

The experiment indicates characteristics of PC material are very sensitive to strain rates and temperatures. Hence, it is necessary to build a physically robust constitutive model to properly describe mechanical behavior of PC varying from low to high rates and temperatures. The rheological interpretation of one-dimensional viscoelastic-viscoplastic model proposed in this paper is illustrated in Fig. 8, aiming to understand rate-dependent thermoelastic and thermoplastic mechanical behavior for PC.

Based upon the experimental results in the section above, this original constitutive model is divided into two parts. The first part, depicting nonlinear viscoelastic response of pre-yield regime, consists of an elastic spring and a dashpot in series, which is the basic model, Maxwell element model, in viscoelasticity theory. The advantage is that it is simply and basic to make the equation very easily understood and conveniently exploited. Nevertheless, distinguishing from the traditional Maxwell model, the Maxwell element proposed here is developed by fully taking effects of strain rate and temperature into account for the components: elastic spring and dashpot, which will be discussed specifically in the next section. Concerning the second part, the phase of viscoplasticity, is made up of softening and hardening spring, which is actually

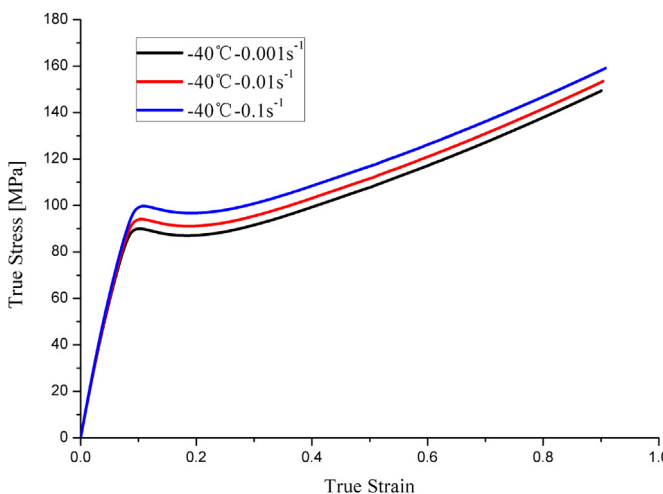


Fig. 5. True stress–true strain curves for PC at -40°C from 0.001 s^{-1} to 0.1 s^{-1} .

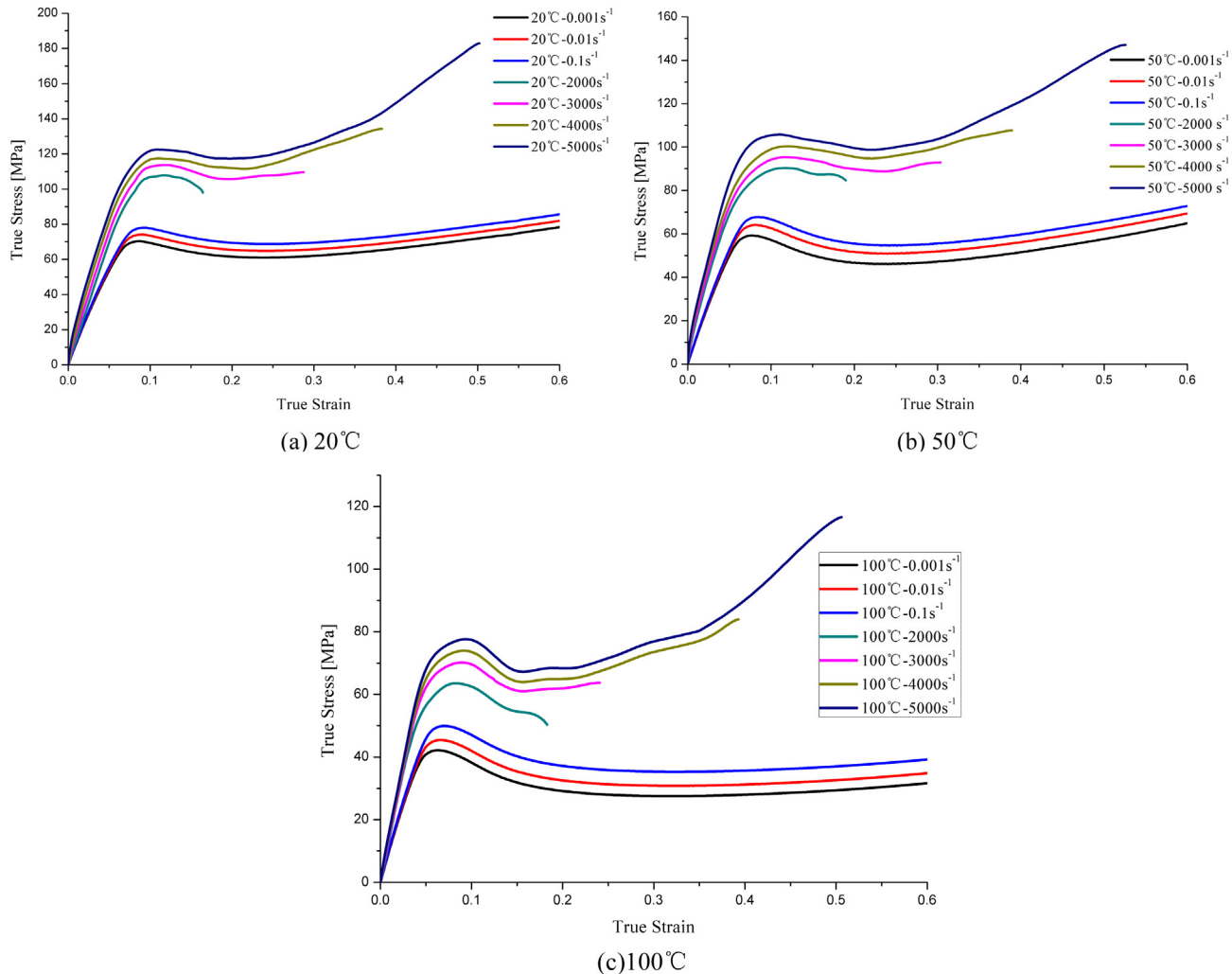


Fig. 6. True stress-true strain curves for PC over 0.001 s^{-1} to 0.1 s^{-1} from low to high rates at three temperatures (a) $20\text{ }^\circ\text{C}$, (b) $50\text{ }^\circ\text{C}$, (c) $100\text{ }^\circ\text{C}$.

presenting conflict and interaction of softening and hardening. In the softening process, our softening model is developed on the basis of the original model proposed by Boyce and Richeton et al. [19,32]. The softening stress is characterized by the integral form of

this developed model. From the aspect of molecular theory, the plastic deformation is attributed to the plastic flow, especially, only when polymer molecular chain segments break through the intermolecular isotropic resistance, do the chain alignments reach

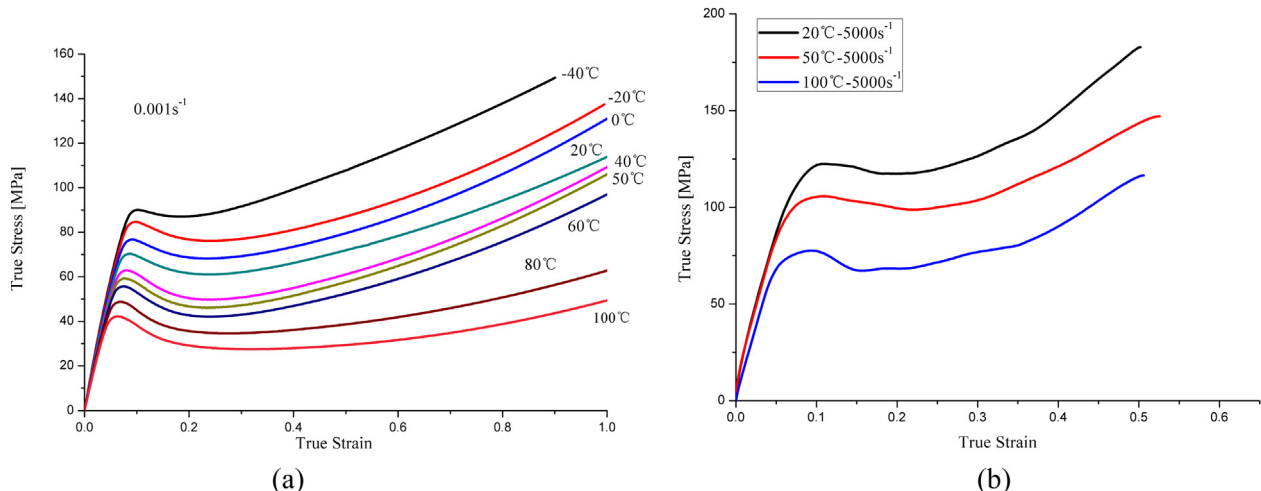


Fig. 7. True stress-true strain curves for PC over wide range of temperatures at different rates. (a) $-40\text{ }^\circ\text{C}$ – $100\text{ }^\circ\text{C}$ at 0.001 s^{-1} ; (b) $20\text{ }^\circ\text{C}$ – $100\text{ }^\circ\text{C}$ at 5000 s^{-1} .

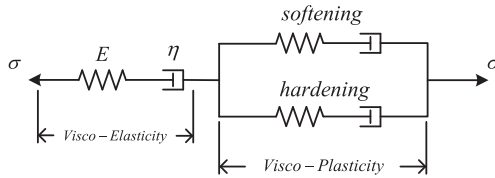


Fig. 8. The rheological description of one-dimensional viscoelastic-viscoplastic constitutive model for PC.

an orientational stable state. The forces to overcome the intermolecular resistance and make the molecular chains rearrangement are the origins for the hardening stress. Our hardening model is established based on the function of a kinematic variable that is used to describe the isotropic hardening for materials in theory of viscoplasticity. When the stress is loaded on the constitutive model in Fig. 8, the viscoelastic deformation e_{ve} would occur in the material with deformation of spring and dashpot in viscoelastic part. While the material comes into the post-yield phase, the interaction of softening and hardening behavior in viscoplastic part would lead to the viscoplastic deformation e_{vp} . Hence, the total deformation of material in our model is equal to sum of viscoelastic and viscoplastic deformation, namely, $e = e_{ve} + e_{vp}$. In brief, the constitutive model we built is intended to focus more on the phenomenological features of PC observed in the experiments from the macroscopic points instead of microscopic points even though some macroscopic mechanical performances are closely associated with the special molecular-level motions. The knowledge on the molecular theory is just used to explain some relevant phenomena and the constitutive model are mainly built up upon the basis of the viscoelastic and viscoplastic theory. Critically, in order to better catch the rate-dependent thermomechanical response of the polycarbonate, the influence by rate and temperature on material

$$\sigma(t) = \int_0^t E\dot{\epsilon}\exp\left(-\frac{t-\theta}{\tau}\right)d\theta \quad (1)$$

Where the E is the Young's modulus of elastic spring, $\tau = \eta/E$ is the relaxation time and η is the viscosity. We would like to point out that despite of quasi-static and dynamic compression load experiment, the $\dot{\epsilon}$ here is the average strain rate over the whole duration of the testing, which is labeled with relevant true stress-true strain curve in Fig. 6 and 7. So when we integrate Eq. (1), we can get

$$\sigma = E\tau\dot{\epsilon}\left[1 - \exp\left(-\frac{\dot{\epsilon}}{\dot{\epsilon}\tau}\right)\right] \quad (2)$$

Eq. (1) is the stress-strain relationship for general Maxwell element. But it is not proper to capture the viscoelastic response for polymer materials. The primary reason is that the Young's modulus E and relaxation time τ are constant and that leads to the limitation of description for the dependence on rate and temperature of polymeric materials. Thus, as long as we regard these two constants as the functions of temperature and strain, we may improve this basic model to understand the viscoelastic property for PC. Firstly, we rewrite Eq. (2) as

$$\sigma_{ve} = E(\dot{\epsilon}, T)\tau(\dot{\epsilon}, T)\dot{\epsilon}\left[1 - \exp\left(-\frac{\dot{\epsilon}}{\dot{\epsilon}\tau(\dot{\epsilon}, T)}\right)\right] \quad (3)$$

Different from the Eq. (2), Young's modulus $E(\dot{\epsilon}, T)$ and relaxation time $\tau(\dot{\epsilon}, T)$ here are assumed to be functions of the absolute temperature T and strain rates $\dot{\epsilon}$. σ_{ve} is the viscoelastic stress. As seen, the next step is to determine the expressions for these two functions. Let us see $E(\dot{\epsilon}, T)$ at first. Richeton et al. [33] improved the original storage modulus model built by Mahieux [44] and then suggested a model for compression modulus of glassy polymers which considers the dependence on temperatures and strain rates:

$$\left\{ \begin{array}{l} E(T, \dot{\epsilon}) = (E_1(\dot{\epsilon}) - E_2(\dot{\epsilon})) \cdot \exp\left(-\left(\frac{T}{T_\beta(\dot{\epsilon})}\right)^{m_\beta}\right) + (E_2(\dot{\epsilon}) - E_3(\dot{\epsilon})) \cdot \exp\left(-\left(\frac{T}{T_g(\dot{\epsilon})}\right)^{m_g}\right) + E_3(\dot{\epsilon}) \cdot \exp\left(-\left(\frac{T}{T_f(\dot{\epsilon})}\right)^{m_f}\right) \\ E_i(\dot{\epsilon}) = E_i^{ref}(\dot{\epsilon}) \cdot (1 + s \cdot \lg(\dot{\epsilon}/\dot{\epsilon}^{ref})), i = \beta, g, f \\ \frac{1}{T_\beta} = \frac{1}{T_\beta^{ref}} + \frac{k}{\Delta H_\beta} \ln\left(\frac{\dot{\epsilon}^{ref}}{\dot{\epsilon}}\right) \\ T_g = T_g^{ref} + \frac{-c_2^g \lg(\dot{\epsilon}^{ref}/\dot{\epsilon})}{c_1^g + \lg(\dot{\epsilon}^{ref}/\dot{\epsilon})} \\ T_f = T_f^{ref} \cdot [1 + 0.01 \cdot \lg(\dot{\epsilon}/\dot{\epsilon}^{ref})] \end{array} \right. \quad (4)$$

parameters is considered sufficiently in the model. This consideration is helpful to improve our model to be valid over a wide range of strain rates and temperature. In the following sections, the model will be discussed in details.

4.1. Viscoelasticity

According to schematic representation of model in Fig. 8, the viscoelastic response is described by a developed Maxwell model. As is known to all, the expression of stress for traditional Maxwell element is

T_β is β -transition temperature, T_g is temperature for glass transition and T_f is the temperature that marks the beginning of the flow region for polymer materials. $E_i(\dot{\epsilon})$ ($i = 1, 2, 3$) is the instantaneous stiffness corresponding to modulus at $T_i(\dot{\epsilon})$ ($i = \beta, g, f$). T_i^{ref} and E_i^{ref} are respectively defined as the transition temperature and instantaneous modulus at reference strain rate. m_i ($i = 1, 2, 3$) is the Weibull moduli, maintaining invariant as constant parameters. k is Boltzmann constant and ΔH_β is the activation energy of the β loss peak. c_1 and c_2 are WLF equation parameters. s can be regarded as sensitivity of strain rate for stiffness modulus. The determined material parameters for proposed storage modulus model are presented in Table 1.

Table 1
Parameters for model of compression modulus proposed by Richeton et al. [33]

Parameters	PC
$\dot{\varepsilon}^{\text{ref}} (\text{s}^{-1})$	1
$E_1^{\text{ref}} (\text{MPa})$	3500
$E_2^{\text{ref}} (\text{MPa})$	1700
$E_3^{\text{ref}} (\text{MPa})$	20
$T_{\beta}^{\text{ref}} (\text{K})$	195
$T_g^{\text{ref}} (\text{K})$	423
$T_f^{\text{ref}} (\text{K})$	436
m_1	5
m_2	80
m_3	15
$\Delta H_{\beta} (\text{kJ/mol})$	40
$c_1 (\text{K})$	289.19
$c_2 (\text{K})$	328.6
s	0.011

The DMA (dynamic mechanical analysis) test is used to monitor storage modulus and loss modulus of materials, which are functions of temperature. Fig. 9 presents the representative DMA test data carried out for PC in this paper at 1 Hz (equal to about 0.04 s^{-1} in compression test according to literature [33]). In particular, the loss modulus reaches peak at around -100°C and 150°C , which indicates the PC undergoes the β -transition and glass transition, respectively. The trend that storage modulus of PC approximately go to zero after 175°C implies PC sample has entered into the flow region. These observations are the same as the work by Boyce [45] and Siviuor [41] and the model proposed by Richeton is also based on this test.

The function of Young's modulus in Eq. (4) has been employed Richeton et al. [10] to describe the elastic behavior for polycarbonate. Even though this model has a reasonable agreement with compression experiment in elastic phase, seen from the Fig. 10(a–c), where the model Eq. (4) and elastic modulus at quasi static compression test in current study has a fair match, it is found that model prediction at high temperature do not perform so excellent as that at low and moderate temperatures since polycarbonate, as a classical type of glassy polymeric material, generally presents viscoelasticity when temperature is high and unfortunately, the model in Eq. (4) fails to catch its viscoelasticity.

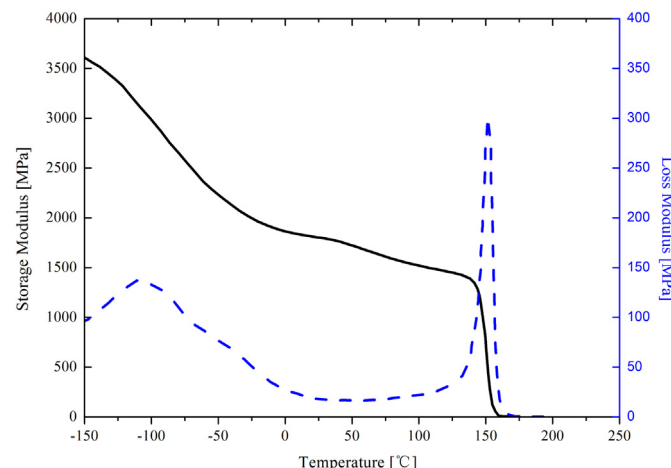


Fig. 9. PC storage modulus and loss modulus as a function of temperature at 1 Hz (about 0.04 s^{-1}).

Nevertheless, the formula in Eq. (4) provides such a physically robust model for Young's modulus that we can directly adopt it as the function $E(\dot{\varepsilon}, T)$ in Eq. (3). As demonstrated in Fig. 10(d), this function is able to give a theoretical prediction for elastic modulus of PC over a wide range of rates. The elastic modulus at low rate is directly obtained from the quasi-static compression test by pulling the tangent modulus from data. While the elastic modulus at high strain rate, due to the fact that the specimen cannot reach the dynamic stress equilibrium state at elastic phase in SHPB experiment, is therefore extrapolated by the model prediction in Eq. (4) based on the DMA test, which shows its predictable ability for elastic modulus varying from low to high rates (up to 10^4 s^{-1}) in Fig. 10(d). The elaborate analysis and discussion has been proceeded by Richeton et al [33], so that we would not go into details.

Therefore, we can get the value of elastic modulus at the specific temperature and strain rate from this model prediction. The subsequent step is to determine the expression for relaxation time $\tau(\dot{\varepsilon}, T)$. At this stage, we assume that $\tau(\dot{\varepsilon}, T)$ is associated to temperature and strain rates as following expression:

$$\tau(\dot{\varepsilon}, T) = \tau_0(T)(\dot{\varepsilon}/\dot{\varepsilon}_0)^{-\beta} \quad (5)$$

Here, the $\tau_0(T)$ is the time parameters which is only dependent on temperature. $\dot{\varepsilon}_0$ is reference strain rate and β is the sensitivity of relaxation time to strain rate. If we take logarithmic form of both sides in Eq. (5), then the evolution can be expressed to Eq. (6):

$$\lg \tau = \lg \tau_0 - \beta \lg(\dot{\varepsilon}/\dot{\varepsilon}_0) \quad (6)$$

Note that the relaxation model we introduce above stems from general mechanical performance of polymer systems that their mechanical property are often sensitive to logarithmic form of strain rate. Simultaneously, the Eq. (6) gives an indication that logarithm of relaxation time and strain rate are linearly connected. Before quantifying β and $\tau_0(T)$, we have to obtain some of relaxation time at different states. To be exact, owing to prediction model for elastic modulus, Eq. (4) is able to be applied to fit true experimental stress–true strain curves in viscoelastic part in Fig. 8. By this way, arbitrary relaxation time in the experimental region of temperature and rate can be obtained. For example, given that the temperature is fixed to 20°C , serials of relaxation time $\tau(20^\circ\text{C}, \dot{\varepsilon})$ could be obtained derived from Eq. (4), displayed in Table 2. As the $\tau_0(T)$ is constant at present, β could be quantified according to linear Eq. (6). Likewise, if we restrict the strain rate to 0.001 s^{-1} , we are also capable of getting the a serial of relaxation time $\tau(T, 0.001 \text{ s}^{-1})$, seen in Table 3. After investigation, the thermal relaxation time variable $\tau_0(T)$ is discovered to be linearly proportional to temperature and the exact expression is given by.

$$\tau_0(T) = 0.1611 - 0.00036T \quad (7)$$

It is important to emphasize that the value of parameter β and the coefficients in Eq. (7) are the averages of all the fitting results based on the experiments and hence they are actually applied crossing all the temperatures and strain rates in experiment. The data in Table 1, Table 2 and Fig. 11 and Fig. 12 are representative. Regardless of that, Observed from Fig. 11 and Fig. 12, it is safe for us to come to a conclusion that the simple developed Maxwell model we suggest, which sufficiently incorporates the reliability of elastic modulus and relaxation time on temperature and rates, is able to reasonably capture mechanical response of polycarbonate in viscoelastic phase. The comparison between the model prediction and experiments can be seen in Section 5 and the furthered discussion and analysis are going to be processed in later section as well.

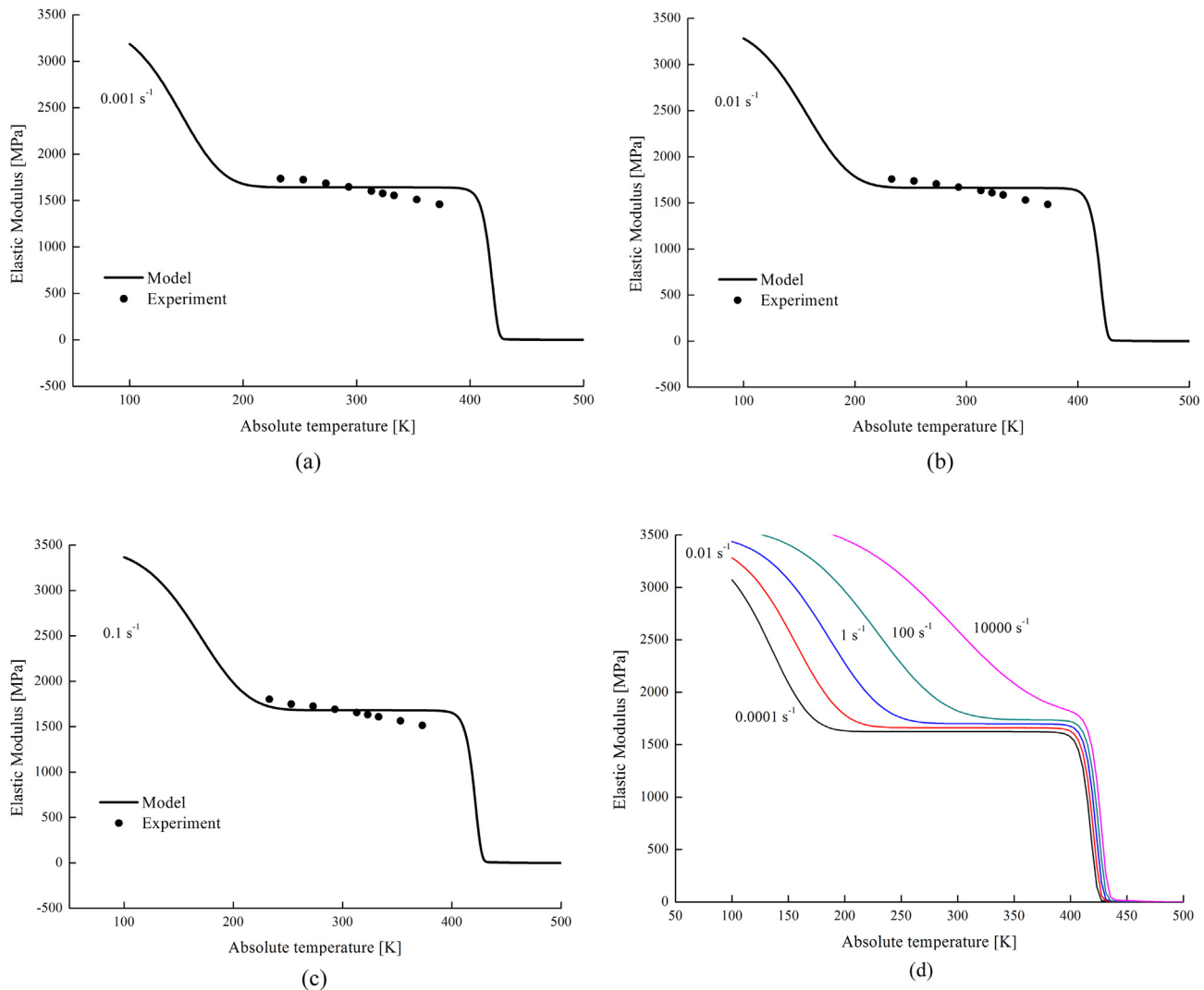


Fig. 10. The comparison of elastic modulus between model prediction and compression test data at low rates. (a) 0.001 s^{-1} ; (b) 0.01 s^{-1} ; (c) 0.1 s^{-1} ; (d) Model prediction for elastic modulus of PC at strain rates from 10^{-4} s^{-1} to 10^4 s^{-1} .

4.2. Yield

Originating from the Ree-Eyring theory [2] and modification of the general Eyring theory [5,17], Boyce et al. found that yield stress of PC increases linearly with the logarithm of strain rate in high and low rates respectively, but what is the more significant is that this material usually undergoes a significant mechanical transition as the strain rate increases beyond a certain critical level that is often located between 10 and 10^3 s^{-1} . This is presented by the remarkable difference between the slope of the yield logarithm of rate in high-

rate regime and that in low-rate regime. This demonstrates the character of PC differentiates prominently from low rate to high rate. In this case, Boyce et al. [19] introduced a decompose-shift-reconstruct (DSR) measurement to decompose the polymeric behavior of PC into α and β process, which is, in practice, is equivalent to the glass g -transition and secondary β -transition as referred above, to understand this noticeable transition for yield behavior. Even though this method allows the model to catch the relationship of yield and logarithm of rate fairly, the DSR measurement would inevitably result in the decomposed-shifted-

Table 2
Value of relaxation time at different rates.

Strain rate (s^{-1})	0.001	0.01	0.1	2000	3000	4000	5000
Relaxation time (s)	55.62	5.82	0.61	2.64×10^{-5}	1.85×10^{-5}	1.46×10^{-5}	1.23×10^{-5}

Table 3
Thermal relaxation time variable from low to high temperatures.

Temperature (K)	233	253	273	293	313	323	333	353	373
Relaxation time (s)	78.46	71.91	62.67	55.62	47.43	43.95	41.02	34.77	29.13

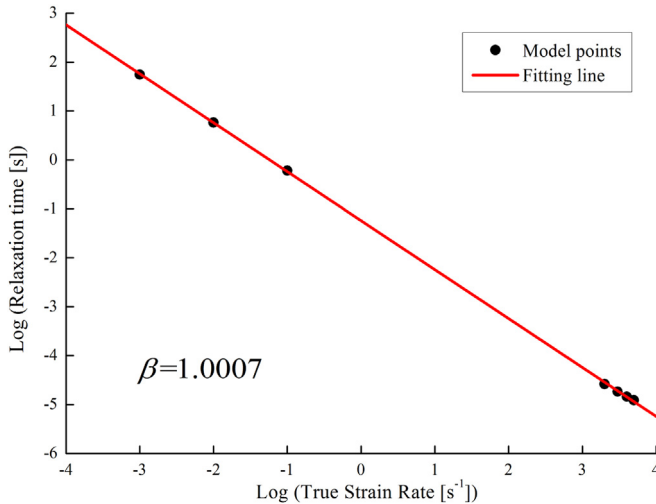


Fig. 11. The linear relationship between logarithm form of relaxation time and true strain rate.

reconstructed behavior in the subsequent post-yield behavior, which could more or less bring some troubles for model creation.

In this section, we intend to use the cooperative model established by Richeton et al. [30] to describe the yield behavior effected by strain rate and temperature. This cooperative model is derived from the acknowledged time–temperature superposition principle, and developed by Richeton [31] to a new formulation of compressive yield stress, which rises with the growth of strain rates and drop of temperature. This formulation reads:

$$\sigma_y = \sigma_i(0) - mT + \frac{2kT}{V} \sinh^{-1} \left(\frac{\dot{\epsilon}}{\dot{\epsilon}_0^* \exp\left(-\frac{\Delta H_\beta}{kT}\right)} \right)^{1/n} \quad (8)$$

Where σ_y is yield stress, $\sigma_i(0)$ is the athermal internal yield stress, m and n are material constants keeping unchanged. $k, T, \dot{\epsilon}, \Delta H_\beta$ is respectively the Boltzmann constant, absolute temperature, strain rate and activation energy as before. V is defined as the activation volume and $\dot{\epsilon}_0^*$ is the invariant pre-exponential rate factor. The way

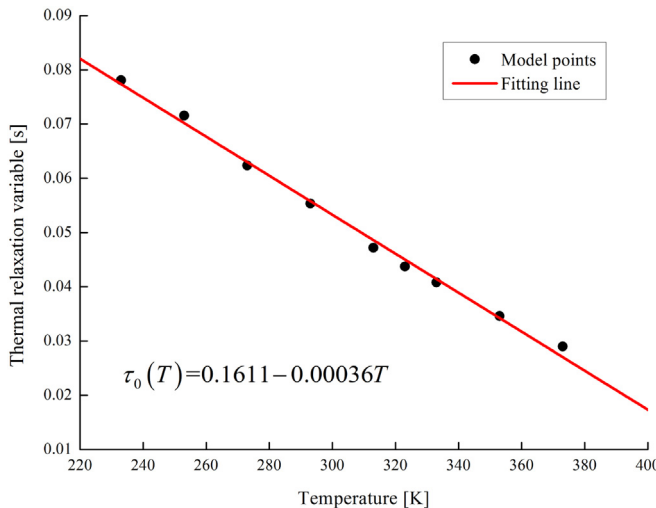


Fig. 12. The linear relationship between thermal relaxation time variable and temperature.

Table 4
Material parameters for cooperative model of ours and Richeton's.

Parameters	Ours	Richeton's
n	3.01	5.88
$V(m^3)$	4.18×10^{-30}	5.16×10^{-29}
$\sigma_i(0)(MPa)$	144.3	145
$m(MPa/K)$	0.24	0.24
$\dot{\epsilon}_0(s^{-1})$	1.64×10^{14}	8.69×10^{12}
$\Delta H_\beta(kJ/mol)$	37.82	40

to determine the these material parameters are explicitly documented in the literature [30,31], so that we would not like to give an unessential explanations here and just present this determined parameters in **Table 4** and the model prediction compared with testing data in **Fig. 13**. The **Fig. 10** displays another version of **Fig. 13** that the true yield stress plays as the function of temperature at $0.001 s^{-1}$, $2000 s^{-1}$ and $5000 s^{-1}$.

As to the yield stress from experiment data, PC sample always performs the strain-softening behavior just after yield point so that the peak stress around 10% strain can be defined as the yield stress. According to formulation of horizontal shifts $\Delta(\log\dot{\epsilon})$ and vertical shifts $\Delta(\sigma_y/T)$ proposed by Richeton et al. [31] and based on the methods on superposition [46,47], the suitable master curve (where the reference temperature is chosen to be $20^\circ C$) is built to hold the yield stress data from experiments, seen in **Fig. 15**. It should be noted that due to the difference in the components and producing process of polycarbonate, the parameters in this article are somewhat different from those in Richeton's work but this diversity is just in a very small scale. Observed from **Figs. 13–15**, the cooperative model exhibits an excellent agreement with experimental yield stress at different rates and temperatures. More critically, this cooperative model is able to cover the sensitivity to rates and temperatures even if PC undergoes an extreme material transition when it comes from low to high rates. That is the primary benefit of this yield-model and the reason why we decide to choose it. Undoubtedly, this model is expected to be tremendously helpful for the construction of the post-yield model.

4.3. Viscoplasticity

As discussed before, the post-yield behavior of PC is actually the interaction and conflict between the strain-softening and strain-

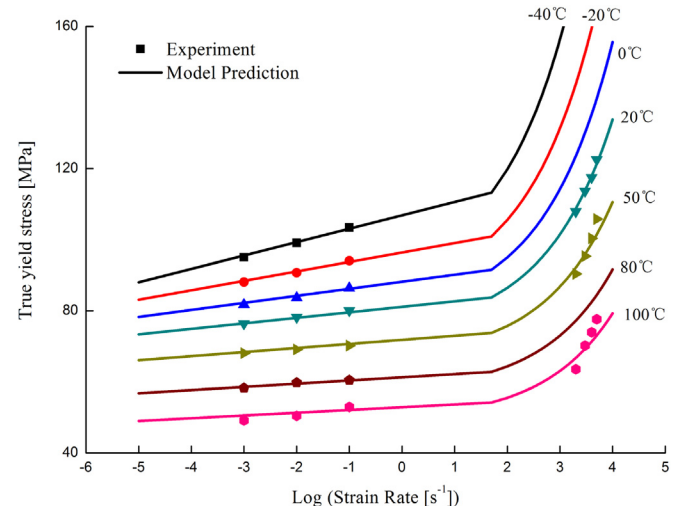


Fig. 13. The comparison of the cooperative model and experiment for true yield stress over a large range of temperature and strain rates.

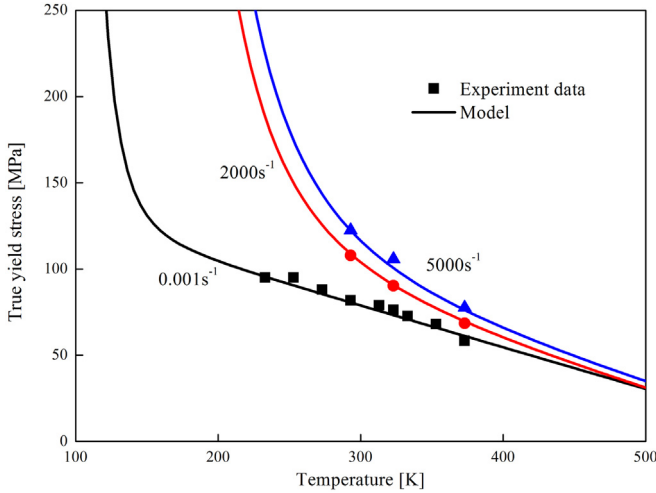


Fig. 14. The comparison of the cooperative model and experiment for true yield stress over a large range of temperature at strain rates 0.001 s^{-1} , 2000 s^{-1} and 5000 s^{-1} .

hardening behavior. On the Basis of this assumption, we propose the viscoplastic stress model, given by.

$$\sigma_{vp} = \sigma_y + \sigma_h - \sigma_s \quad (9)$$

Where the σ_{vp} is viscoplastic stress, σ_y is yield stress and it is expressed the same as Eq. (8). σ_h and σ_s is respectively the hardening stress and softening stress. In order to enable the formulation of hardening stress and softening stress deduced smoothly, we convert the Eq. (8) into

$$\sigma_{vp} = \sigma_y(1 + \bar{\sigma}_h - \bar{\sigma}_s) \quad (10)$$

$\bar{\sigma}_h = \sigma_h/\sigma_y$ and $\bar{\sigma}_s = \sigma_s/\sigma_y$ is the dimensionless form of hardening stress and softening stress. In the following part, we intend to go into further study on these two behaviors.

4.3.1. Softening

The strain-softening behavior of polymer material is generally considered to be caused by shear internal resistance. The softening original model is built by Boyce et al. [4] and afterward made evolutions by Boyce [19] and Richeton [32]. The improved model is written as.

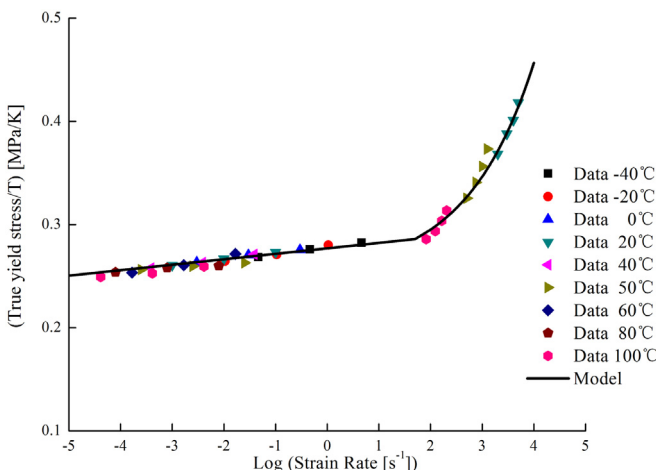


Fig. 15. Master curve built at $20\text{ }^\circ\text{C}$ for comparison with the yield stress over wide rates and temperature in the uniaxial compression test.

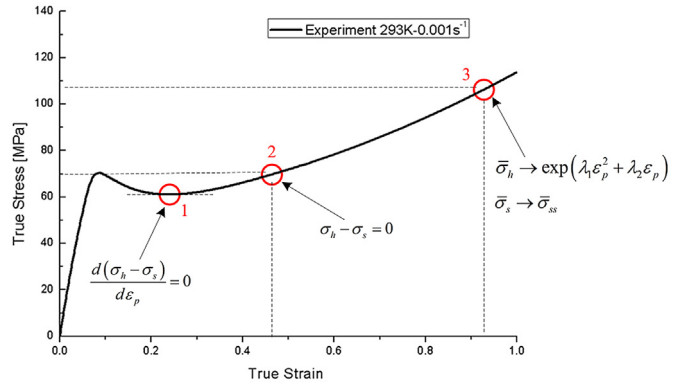


Fig. 16. The true stress-strain curve at $20\text{ }^\circ\text{C}$ and 0.001 s^{-1} used for identification of parameters for viscoplastic stress model.

$$\dot{s} = h \left(1 - \frac{s}{s_{ss}} \right) \dot{\gamma}^p \quad (11)$$

Where s is the athermal shear stress, expected to evolve with the plastic shear strain γ^p until to achieve a preferred stable state, s_{ss} . h is the softening slope and keep constant during the loading procedures. According to the Von Mises yield criterion, the relationship between effective yield stress σ_{ey} and shear yield stress τ_{sy} is defined as $\sigma_{ey} = \sqrt{3}\tau_{sy}$. As the effective stress is equal to uniaxial compression stress in the uniaxial compression experiments, it allow us to approximately assume that relation between effective plastic compression stress σ_p and plastic shear stress τ_p still follows as $\sigma_p = \sqrt{3}\tau_p$ at post-yield stage. Based on the research in literature [31], the pre-exponential effective rate factor $\dot{\epsilon}_0$ is able to be written as the function of the pre-exponential shear rate factor $\dot{\gamma}_0$ and Poisson's rate ν , $\dot{\epsilon}_0 : \dot{\gamma}_0 = (2\sqrt{3}/3)(1 + \nu) \approx \sqrt{3}$. Thus, the correction of the softening model in Eq. (11) is deduced to

$$\dot{\sigma}_s = h \left(1 - \frac{\sigma_s}{\sigma_{ss}} \right) \dot{\epsilon}_p \quad (12)$$

Here, the σ_s is the softening stress in the uniaxial compression test, σ_{ss} is preferred stable state for σ_s , and $\dot{\epsilon}_p$ is the effective plastic strain rate. Because the softening stress has the similar characteristic as the internal stress, which is always linearly proportional to the temperature T , incorporated the hydrostatic pressure, the expression of σ_{ss} can be assumed as.

$$\sigma_{ss} = P + \alpha_0 T \quad (13)$$

Where P is pressure, α_0 is the thermal coefficient. Based on the this strain-softening model, a dimensionless formulation for softening for can be introduced that

Table 5
Parameters for viscoplastic constitutive model.

Parameters	PC
$\dot{\epsilon}^{ref}(\text{s}^{-1})$	0.001
λ_1^{ref}	0.38
λ_2^{ref}	0.19
$\lambda_3^{ref}(K)$	1047
s_1	1.42×10^{-3}
s_2	4.92×10^{-3}
s_3	7.96×10^{-5}
\bar{P}	0.003
$\alpha(K^{-1})$	7.5×10^{-3}
\bar{h}	5.58
q	0.52

$$\begin{cases} \dot{\bar{\sigma}}_s = \bar{h} \left(1 - \frac{\bar{\sigma}_s}{\bar{\sigma}_{ss}} \right) \dot{\varepsilon}_p \\ \bar{\sigma}_{ss} = \bar{P} + \alpha T \end{cases} \quad (14)$$

The physical quantities in original equation have been corrected to be dimensionless, though, their physical interpretations and representations are not altered. It is clear that Eq. (12) demonstrates softening stress σ_s and plastic strain rate $\dot{\varepsilon}_p$ have the same dependence on rate. Since they are both the derivative of time, we can change Eq. (14) into.

$$\frac{d\bar{\sigma}_s}{d\varepsilon_p} = \bar{h} \left(1 - \frac{\bar{\sigma}_s}{\bar{\sigma}_{ss}} \right) \quad (15)$$

Integral Eq. (14) with ε_p and employ the initial condition, the starting point at post-yield phase, namely, the yield point where $\dot{\varepsilon}_p = 0$ and $\sigma_s = \bar{\sigma}_s = 0$. Then we can obtain.

$$\begin{cases} \sigma_{vp} = \sigma_y \left(1 + \exp(\lambda_1 \varepsilon_p^2 + \lambda_2 \varepsilon_p) \left[1 - \exp\left(-\frac{\lambda_3}{T} \varepsilon_p\right) \right] - \bar{\sigma}_{ss} \left[1 - \exp\left(-\frac{\bar{h}}{\bar{\sigma}_{ss}} \varepsilon_p\right) \right] \right) \\ \bar{\sigma}_{ss} = \bar{P} + \alpha T \\ \lambda_i^{ref} - 1 = s_i \left[\left(\frac{\dot{\varepsilon}}{\dot{\varepsilon}_{ref}} \right)^q - 1 \right], \quad i = 1, 2, 3 \end{cases} \quad (20)$$

$$\bar{\sigma}_s = \bar{\sigma}_{ss} \left[1 - \exp\left(-\frac{\bar{h}}{\bar{\sigma}_{ss}} \varepsilon_p\right) \right] \quad (16)$$

This equation indicates that softening stress σ_s actually increases with growth of plastic strain ε_p of material and then gradually reaches the structure stable stress σ_{ss} when the plastic deformation becomes larger enough. This trend accords with the evidence that the stress of PC often undergoes a dramatic drop after the yield point from the phenomenological observations, which results from drastic rise of softening stress caused by the rearranging of molecular chain segments in microstructure.

4.3.2. Hardening

When the materials begin to access to the hardening phase, tangent modulus is usually found to increase. In terms of these materials, according to viscoplastic theory, the function $\Phi(p)$ is often incorporated into the kinematic variable to describe the isotropy oriental hardening behavior for material. $\Phi(p)$ is expressed as.

$$\Phi(p) = \Phi_s + (1 - \Phi_s)e^{-\omega p} \quad (17)$$

It is found that with the increase of p and $\Phi(p)$ would finally get close to its initial value Φ_s . Take advantage of the feature of this function, we set up the dimensionless formulation for hardening stress. $\bar{\sigma}_h$

$$\bar{\sigma}_h = \exp(\lambda_1 \varepsilon_p^2 + \lambda_2 \varepsilon_p) \left[1 - \exp\left(-\frac{\lambda_3}{T} \varepsilon_p\right) \right] \quad (18)$$

where $\lambda_i(1,2,3)$ are the hardening material parameters. It deserves to notice that if $\lambda_i(1,2,3)$ were remaining invariant over the duration of the whole plastic deformation, then the hardening behavior would not be rate dependent. However, from the compression

experiments in Fig. 7, it is indicated apparently that hardening rate and degree at high rate regime is much more sharply than that at low rates. So the ignorance of the rate dependence on hardening material parameters may likely lead to limitations for the extent application of the constitutive model. For this case, it is supposed to regard $\lambda_i(1,2,3)$ as the functions of strain rate. In order to enable model in Eq. (18) cover hardening response of PC material on a large scale, we intend to accord with the elastic modulus model established in Eq. (4) and design a similar formulation of $\lambda_i(1,2,3)$ based upon the reference strain rate:

$$\frac{\lambda_i}{\lambda_i^{ref}} - 1 = s_i \left[\left(\frac{\dot{\varepsilon}}{\dot{\varepsilon}_{ref}} \right)^q - 1 \right], \quad i = 1, 2, 3 \quad (19)$$

λ_i^{ref} is the material parameter at reference strain rate $\dot{\varepsilon}_{ref}$. s_i is the sensitive quantity for the given polymer and q is the exponential constant. At this point, the viscoplastic stress model at phase of plastic deformation is able to be denoted as:

$$\bar{\sigma}_s = \bar{\sigma}_{ss} \left[1 - \exp\left(-\frac{\bar{h}}{\bar{\sigma}_{ss}} \varepsilon_p\right) \right] \quad (20)$$

As shown in equation, there are total 7 material parameters required to be quantified. They are $s_i(1,2,3)$, q , \bar{h} , \bar{P} , α . However, after carefully investigating the Eq. (20), it is observed that, in case that λ_i at two different rates were determined, the s_i and q would be figured out. So as the situation for $\bar{\sigma}_{ss}$ that the determination of $\bar{\sigma}_{ss}$ at two different temperatures would make \bar{P} and α identified. As a matter of fact, provided that the value of 0.001 s^{-1} is taken as the reference strain rate and the true stress-strain curve at 20°C , 0.001 s^{-1} is regarded as reference curve, then what supposed to be ascertained in Eq. (20) are five parameters $\lambda_i(0.001 \text{ s}^{-1})$, $i = 1, 2, 3$, \bar{h} and $\bar{\sigma}_{ss}(20^\circ\text{C})$. So the first step is to pick up the stress-strain curve at 20°C , 0.001 s^{-1} as follow:

As shown in Fig. 16, the three points marked on the curve are specially meaning. As we know, at the moment that PC material comes into the viscoplastic phase, on account of the breaks of the original molecule alignment and rearrangement of new molecular chain segment, the strain-softening behavior and hardening behavior both occur simultaneously. Before the stress reaches the point 2, the softening stress increase more evidently than hardening stress and viscoplastic stress touches the bottom at point 1 (extreme value), which means $\frac{d(\sigma_h - \sigma_s)}{d\varepsilon_p} = 0$. Later on, when the viscoplastic stress arrives at point 2, where there is $\sigma_h - \sigma_s = 0$, indicating that growth rate of softening stress slows down while hardening stress goes up more rapidly from point 1 to point 2. Afterward, the dimensionless softening stress $\bar{\sigma}_s$ gradually approaches to its preferred stable state $\bar{\sigma}_{ss}$ at final point 3, where the plastic deformation of PC material is large enough. In contrast, the dimensionless hardening stress shows a dramatic upward trend over this duration and accesses to its steady growth function as $\exp(\lambda_1 \varepsilon_p^2 + \lambda_2 \varepsilon_p)$. This analysis process allows us to construct the equations to figure out those 5 parameters. Specifically, as $\bar{\sigma}_s$ and $\bar{\sigma}_h$ around the point 3 has been respectively simplified to $\bar{\sigma}_{ss}$ and

$\exp(\lambda_1 \varepsilon_p^2 + \lambda_2 \varepsilon_p)$, the 3 groups of stress-strain points around the point 3 can be chosen to substitute into the first equation in Eq. (20). By solving these three equations, $\lambda_1(0.001 \text{ s}^{-1})$, $\lambda_2(0.001 \text{ s}^{-1})$, $\bar{\sigma}_{ss}(20^\circ\text{C})$ can be obtained. Combined with the equations built at point 1 and point 2:

$$\begin{cases} \frac{d(\sigma_h - \sigma_s)}{d\varepsilon_p} = 0 \\ \sigma_h - \sigma_s = 0 \end{cases} \quad (21)$$

Then the $\lambda_3(0.001 \text{ s}^{-1})$, \bar{h} can be obtained as well. Subsequently, we select another true stress-strain curve at different strain rate and temperature such as $(80^\circ\text{C}, 0.1 \text{ s}^{-1})$, following the same steps above, and we can get $\lambda_1(0.1 \text{ s}^{-1})$, $\lambda_2(0.1 \text{ s}^{-1})$, $\lambda_3(0.1 \text{ s}^{-1})$, $\bar{\sigma}_{ss}(80^\circ\text{C})$. With $\lambda_i(\dot{\varepsilon})$ and $\bar{\sigma}_{ss}(T)$ at $(20^\circ\text{C}, 0.001 \text{ s}^{-1})$ and $(80^\circ\text{C}, 0.1 \text{ s}^{-1})$, connected the second and third equations in Eq. (20), the left parameters s_i , q , α , \bar{P} can be quantified. The determined material parameters for viscoplastic constitutive model of PC are listed in Table 4.

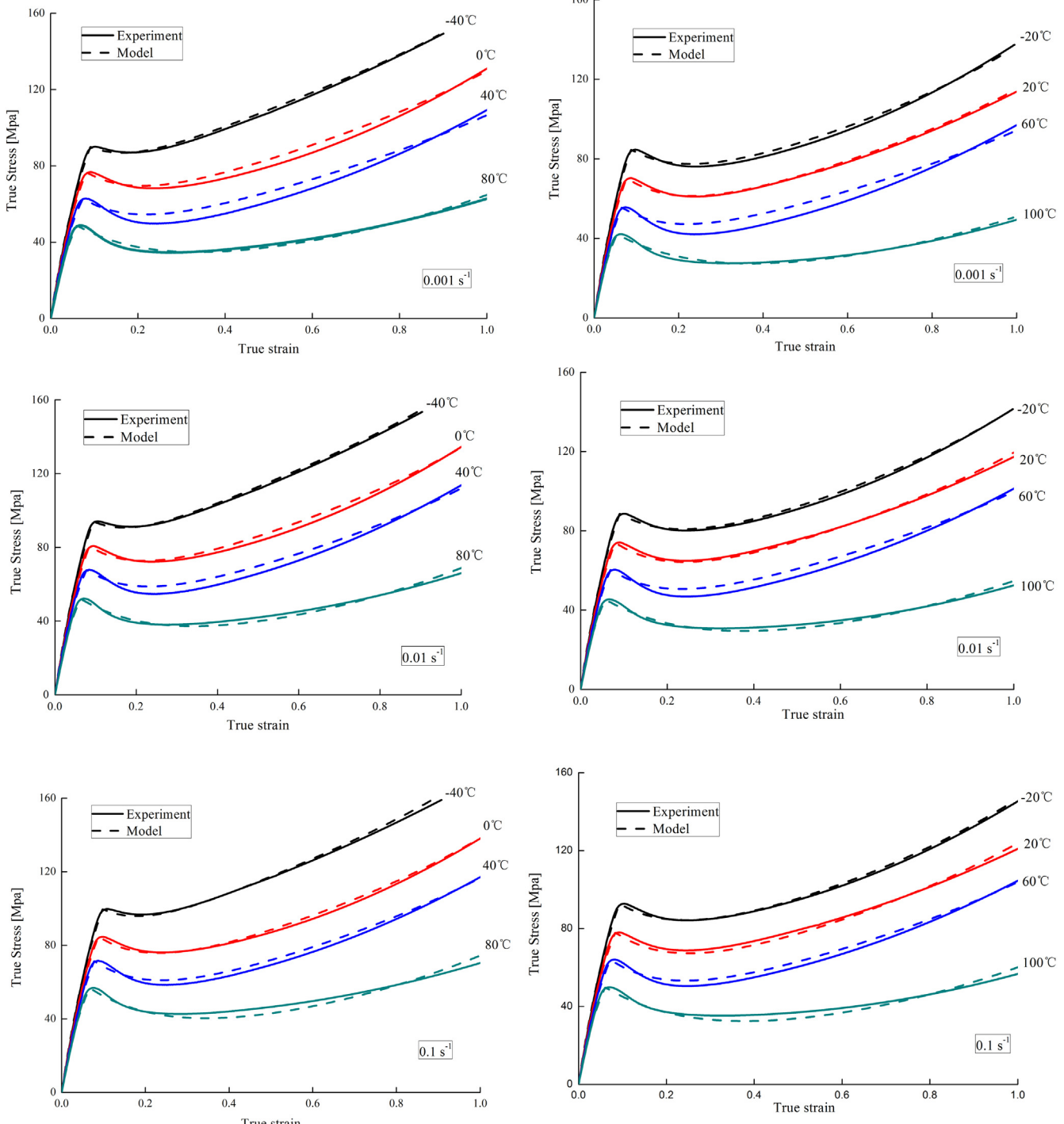


Fig. 17. The validation of the constitutive model by comparing the model prediction with the uniaxial compression experiments from low to high strain rates and temperatures.

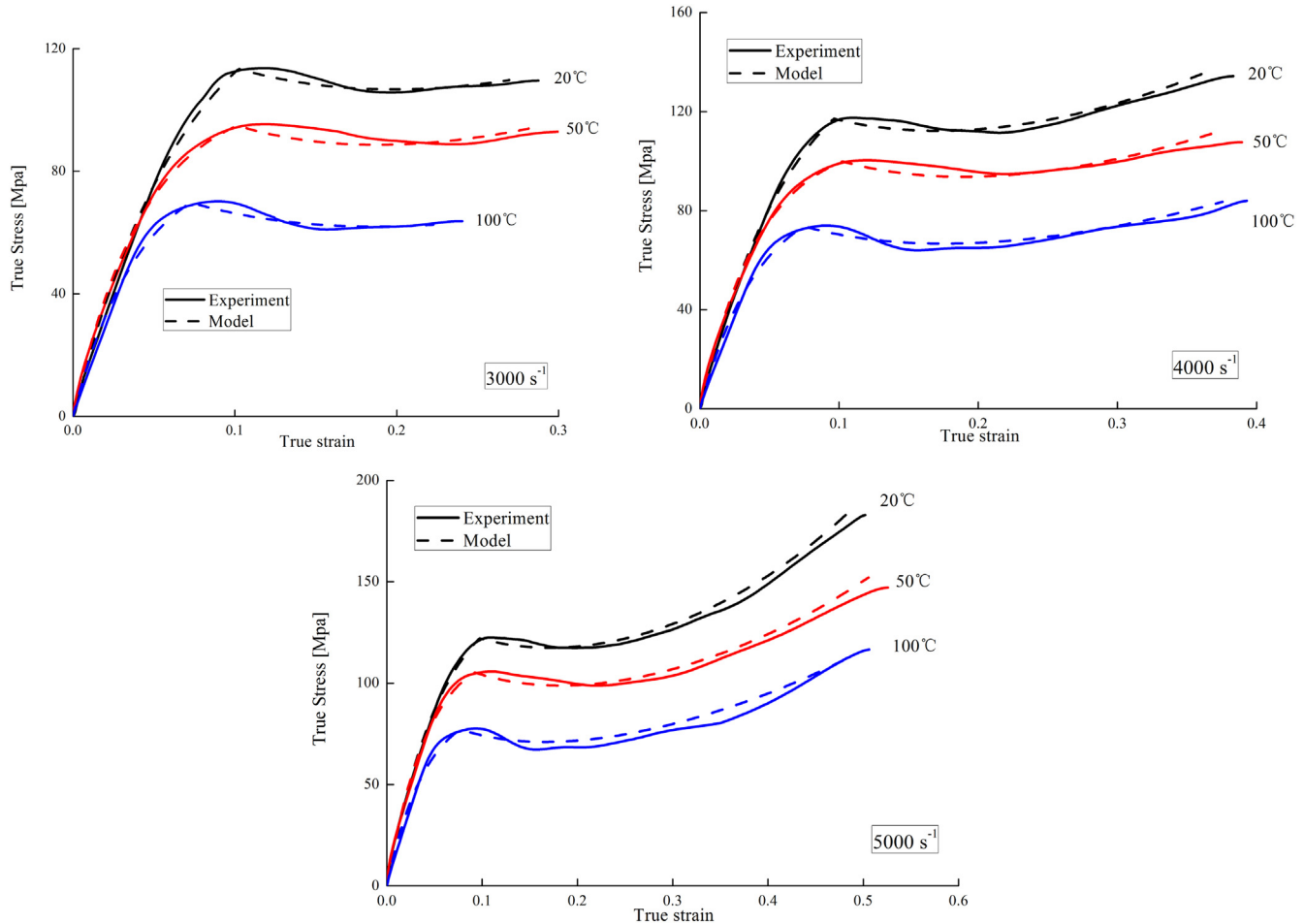


Fig. 17. (continued).

It is worth noting that although the two true stress-strain curves are adequate enough to determine these material constants, but to be more accurate and reasonable, several experimental curves over a wide range of strain rates and temperatures are adopted so that the parameters in Table 5 are experimental average values. At this stage, the intact one-dimensional visco-elastic and visco-plastic constitutive model for polycarbonate has been completely derived:

5. Model vs experiment and analysis

The comparisons between constitutive model prediction and experimental result are demonstrated in Fig. 17 and the Fig. 19 shows the comparison between experiments and Boyce model [19] and Richeton model [32]. Compared with model proposed by Boyce and Richeton, it is remarkable that no matter in elastic phase

$$\sigma = \begin{cases} E\tau \left(1 - e^{-\frac{\dot{\epsilon}}{\dot{\epsilon}\tau}}\right), & \sigma < \sigma_{yield} \\ \sigma_i(0) - mT + \frac{2kT}{V} \sinh^{-1} \left(\frac{\dot{\epsilon}}{\dot{\epsilon}_0^* \exp\left(-\frac{\Delta H_\beta}{kT}\right)} \right)^{1/n}, & \sigma = \sigma_{yield} \\ \sigma_y \left(1 + \exp\left(\lambda_1 \epsilon_p^2 + \lambda_2 \epsilon_p\right) \left[1 - \exp\left(-\frac{\lambda_3}{T} \epsilon_p\right)\right] - \bar{\sigma}_{ss} \left[1 - \exp\left(-\frac{\bar{h}}{\bar{\sigma}_{ss}} \epsilon_p\right)\right]\right), & \sigma > \sigma_{yield} \end{cases} \quad (22)$$

The explicit expressions and explanations for relevant material constants have been discussed in sections above, and all the values of these parameters have been listed in Tables 1–5.

and plastic phase, our constructed visco-elastic and visco-plastic model performs better agreements with data in compression tests over a wide range of strain rates and temperatures. The

standard errors between the model prediction and data are calculated, where the error bound is less than 7% and some matches even reach at almost 98%.

Firstly, it is very obvious that our model perfectly characterizes the testing data for PC in elastic phase no matter in high or low rates and temperatures, seen from the Fig. 18. That is because our model incorporates viscoelastic behavior by employing the improved Maxwell element, which is more precise to describe the non-linear stress-strain relationship of polymer material than just

using elastic modulus functions in Eq. (4) proposed by Richenton [34]. That also indicates that mechanical response of PC in elastic regime are sensitive to temperature and strain rate.

Secondly, the cooperative model for depiction of yield stress plays a significant role in link with pre-yield and post-yield behavior. It guarantees that PC material experiences smoothly from elastic to plastic regime without any skip and meanwhile this formulation well catches the dependence on strain rates and temperatures of yield response.

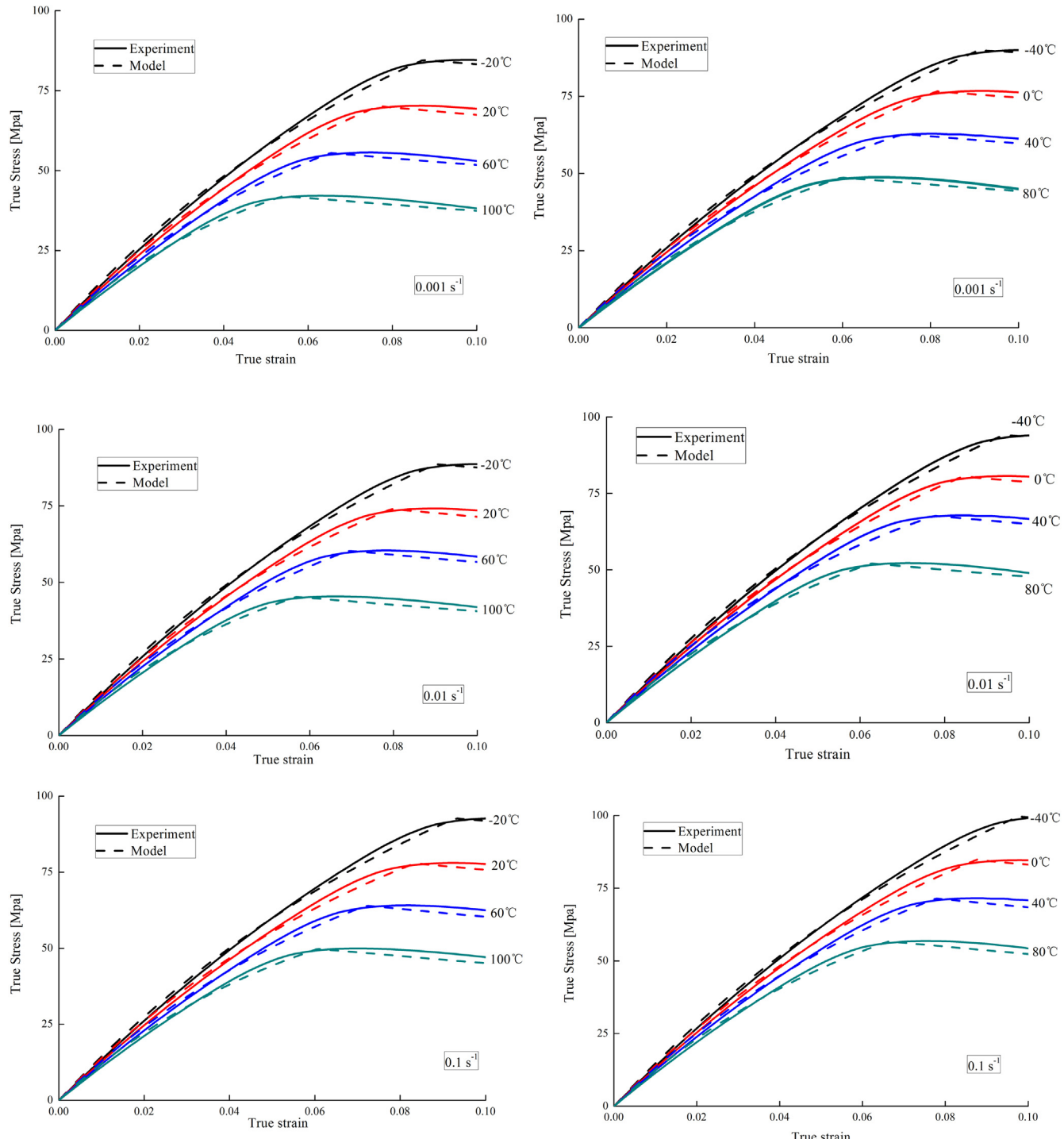


Fig. 18. The validation of the constitutive model by comparing the model prediction with the uniaxial compression experiments from low to high strain rates and temperatures at strain range from (0–0.1).

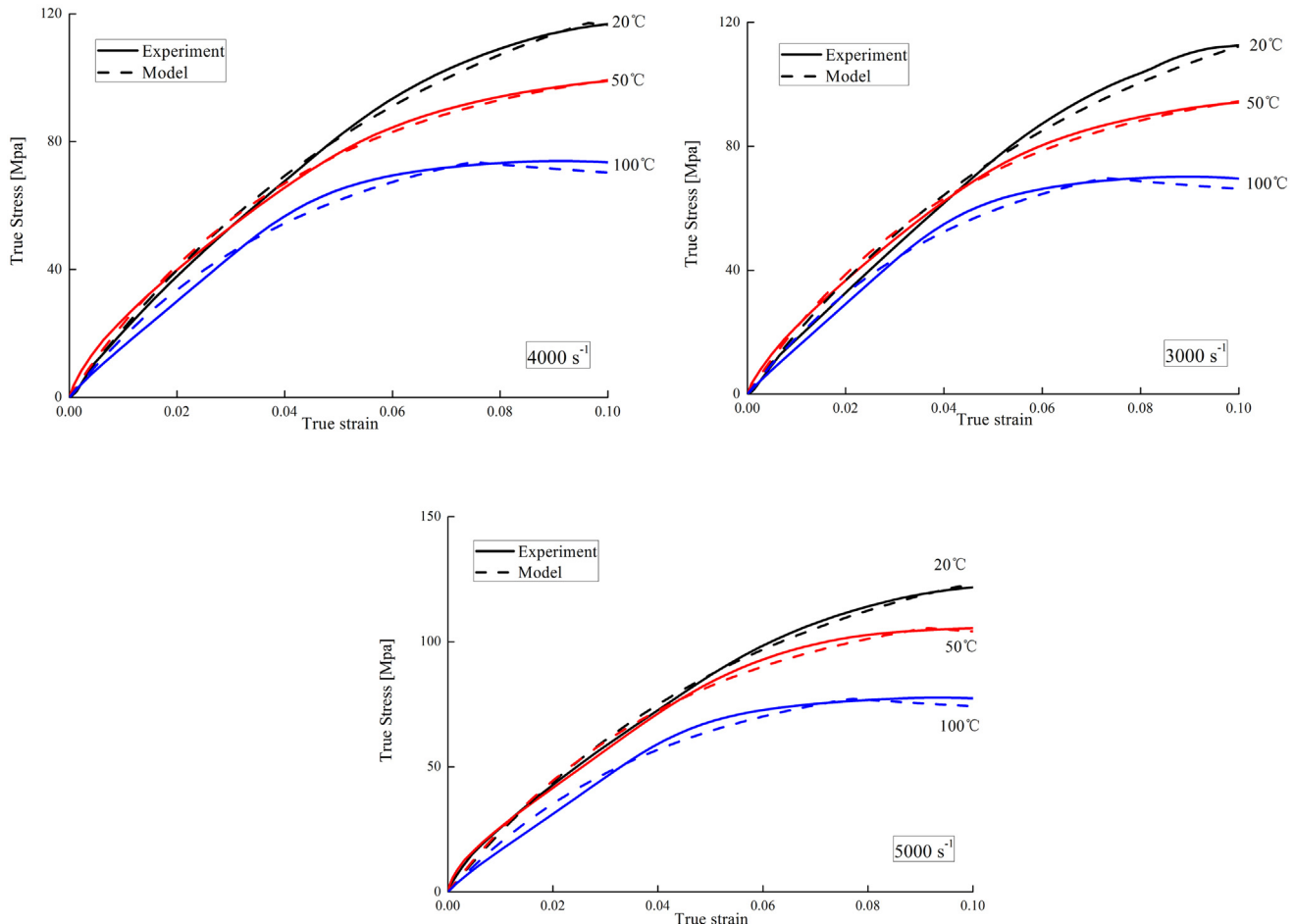


Fig. 18. (continued).

Furthermore, our visco-plastic model that introduces the concept of interaction and conflict with softening and hardening behavior, is definitely proved to exactly present the phenomenological observations in experiments. After yield point, the strain-softening phenomenon occurs at first and soon leads to the lowest stress in PC material structure. That indicates softening behavior currently dominates the fight with softening behavior.

Afterward, the softening stress gradually reaches a steady state whereas the hardening stress rises with a sharp rate. Beyond the specific point (point 3 in Fig. 16), where these two stress are equal to each other, the hardening behavior begins to be the charged of this conflict and eventually predominates completely. In addition, by investigating on experiment results, we can discover that softening response is much more sensitive to temperature and yet

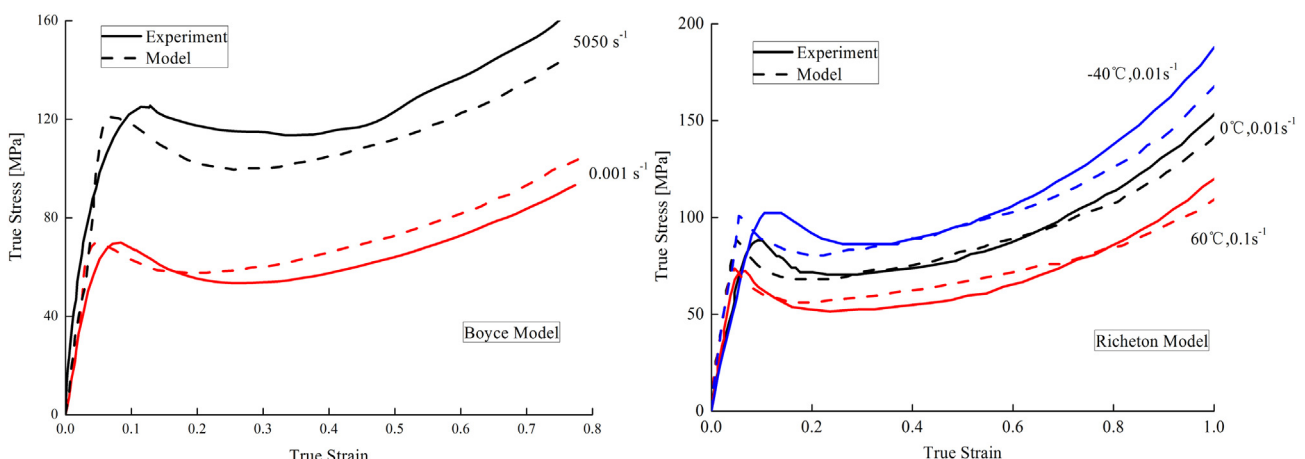


Fig. 19. The comparisons with the experiments by Boyce model [19] and Richeton model.[32].

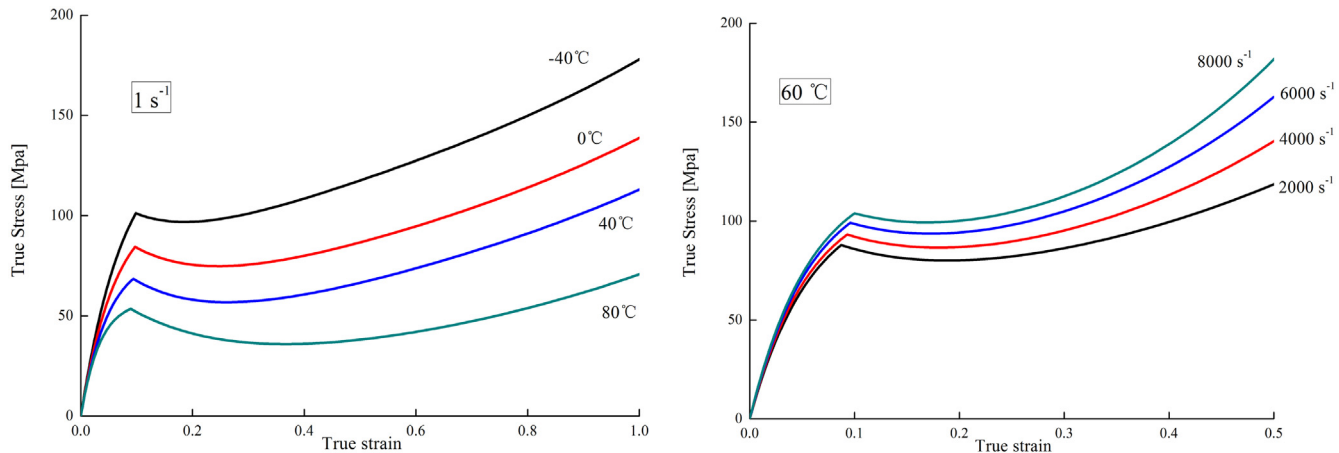


Fig. 20. The model prediction of the true stress-true strain curves at 0.1 s^{-1} from -40°C to 80°C and 60°C from 2000 s^{-1} to 8000 s^{-1} .

hardening response is chiefly affected by strain rate. That is in accordance with our model in Eq. (20) that dimensionless softening stress is mainly the function of temperature while hardening stress increases with exponential of strain rates. Hence, it is found that softening behavior performs more apparently in high temperature, but in very high rate (5000 s^{-1}), the softening phenomenon seems to almost disappear. Instead, PC directly performs exponential hardening just after yield and goes up to very high stress. More exactly speaking, that is due to the so much drastic hardening behavior that covers the softening behavior rather than the too weakness of softening behavior.

In order to present the extension and predictable availability of the established constitutive model, the prediction of true stress-true strain curves at 0.1 s^{-1} from -40°C to 80°C and 60°C from 2000 s^{-1} to 8000 s^{-1} are respectively made in the Fig. 20. Compared with the results in Fig. 17, the predictable curves also perfectly characterize the rate-dependent and thermomechanical property of PC material in both elastic and plastic regime, which makes our model further validation.

6. Conclusion

In this paper, a combined experimental and analytical investigation has been presented to understand the rate-dependent thermomechanical characteristics of polycarbonate over a large range of strain rates and temperatures. A one-dimensional robust physically consistent viscoelastic and viscoplastic constitutive model is established. At elastic stage, a developed Maxwell model is proposed, in which the elastic modulus is used by the model suggested by Richeton [34], and the relaxation time is defined as the function of strain rates and temperatures. The improvement overcomes the weakness that only employing the elastic modulus is not capable of fully covering the non-linear viscoelastic behavior of polymer materials. The yield stress is presented by cooperative model, which properly makes connection with pre-yield and post-yield mechanical behavior. When PC comes into the plastic deformation, a viscoplastic stress model is set up and the dimensionless measurements for softening and hardening stress certainly brings about the convenience for the model derivation and parameter definition. In order to expand our model to wider application at a large region of rates and temperatures, the main parameters in model are sufficiently constructed as the functions of rates and temperatures. Although, by this way, the more material constants are unavoidably involved into model, these quantities are so well-defined that they are able to be identified right from experiments

or simple calculations instead of being much reliable on fitting or iteration methods, which means our constitutive model are profoundly physical based. Furthermore, the remarkable and reasonable agreement between the model prediction and experimental results makes the effective validation for the constitutive model. Finally, we would like to point out that the visco-elastic and viscoplastic model for polycarbonate established in present paper is given to the explicit relationship between the stress and strain. One of the benefit is that the material parameters can be identified before implementation of model into Finite Element Method (FEM). This way is able to provide the initial value of material constants for iteration in FEM, which is advantage for the better convergence and accuracy in numerical method. Certainly, this robust physically constitutive model based on the phenomenological observations is undoubtedly the first step toward the depiction for the mechanical response of the polymer materials over a wide range of strain rates and temperatures. Also, the applications of this model for the tensile behavior of other polymeric materials and the its verifications on the structure experiments are going to be further investigated in the following work.

Acknowledgments

The financial sponsorship and support from the Natural Science Foundation of China (Grant Nos. 11372113 and 11472110) and International Scientific and Technological Cooperation and Special Projects (NO.2011DFA53080) are greatly appreciated. This work also benefits from independent research of State Key Laboratory of Sub-tropical Building Science (2014ZC18). This paper is also supported by the opening project of State Key Laboratory of Explosion Science and Technology (Beijing Institute of Technology) (KJJ14-2M).

References

- [1] Haward RN, Thackray G. The use of a mathematical model to describe isothermal stress-strain curves in glassy thermoplastics. Proc R Soc Lond Ser A, Math Phys Sci 1968;302(1471):453–72.
- [2] Eyring H. Viscosity, plasticity, and diffusion as examples of absolute reaction rates. J Chem Phys 1936;4(4):283–91.
- [3] Arruda EM, Boyce MC. Evolution of plastic anisotropy in amorphous polymers during finite straining. Int J Plasticity 1993;9(6):697–720.
- [4] Boyce MC, Parks DM, Argon AS. Large inelastic deformation of glassy polymers. part I: rate dependent constitutive model. Mech Mater 1988;7(1): 15–33.
- [5] Hasan OA, Boyce MC, Li XS, Berko S. An investigation of the yield and post yield behavior and corresponding structure of poly(methyl methacrylate). J Polym Sci Part B: Polym Phys 1993;31(2):185–97.
- [6] Buckley CP, Jones DC. Glass-rubber constitutive model for amorphous polymers near the glass transition. Polymer 1995;36(17):3301–12.

- [7] De Focatiis DSA, Embrey J, Buckley CP. Large deformations in oriented polymer glasses: experimental study and a new glass-melt constitutive model. *J Polym Sci Part B: Polym Phys* 2010;48(13):1449–63.
- [8] Wu JJ, Buckley CP. Plastic deformation of glassy polystyrene: a unified model of yield and the role of chain length. *J Polym Sci Part B: Polym Phys* 2004;42(11):2027–40.
- [9] Govaert LE, Timmermans PHM, Brekelmans WAM. The influence of intrinsic strain softening on strain localization in polycarbonate: modeling and experimental validation. *Am Soc Mech Eng* 2000;122(2):177–85.
- [10] Klompen ETJ, Engels TAP, Govaert LE, Meijer HEH. Modeling of the post yield response of glassy Polymers: influence of thermomechanical history. *Macromolecules* 2005;38(16):6997–7008.
- [11] Tervoort TA, Smits RJM, Brekelmans WAM, Govaert LE. A constitutive equation for the elasto-viscoplastic deformation of glassy polymers. *Mech Time-Depend Mat* 1997;1(3):269–91.
- [12] Tervoort TA, Govaert LE. Strain-hardening behaviour of polycarbonate in the glassy state. *J Rheol* 2000;44(6):1263–77.
- [13] van Melick HGH, Govaert LE, Meijer HEH. On the origin of strain hardening in glassy polymers. *Polymer* 2003;44(8):2493–502.
- [14] Wendlandt M, Tervoort TA, Suter UW. Non-linear, rate-dependent strain-hardening behavior of polymer glasses. *Polymer* 2005;46(25):11786–97.
- [15] Wendlandt M, Tervoort TA, Suter UW. Strain-hardening modulus of cross-linked glassy poly(methyl methacrylate). *J Polym Sci Part B: Polym Phys* 2010;48(13):1464–72.
- [16] Wu PD, Van Der Giessen E. On improved network models for rubber elasticity and their applications to orientation hardening in glassy polymers. *J Mech Phys Solids* 1993;41(3):427–56.
- [17] Ree T, Eyring H. Theory of non-Newtonian flow. I. Solid plastic system. *J Appl Phys* 1955;26(7):793–800.
- [18] Bauwens JC. Relation between the compression yield stress and the mechanical loss peak of bisphenol-A-polycarbonate in the β transition range. *J Mater Sci* 1972;7(5):577–84.
- [19] Mulliken AD, Boyce MC. Mechanics of the rate-dependent elastic-plastic deformation of glassy polymers from low to high strain rates. *Int J Solids Struct* 2006;43(5):1331–56.
- [20] Safari KH, Zamani J, Ferreira FJ, Guedes RM. Constitutive modeling of polycarbonate during high strain rate deformation. *Polym Eng Sci* 2013;53(4):752–61.
- [21] Varghese AG, Batra RC. Constitutive equations for thermomechanical deformations of glassy polymers. *Int J Solids Struct* 2009;46(22–23):4079–94.
- [22] van Bremen LCA, Klompen ETJ, Govaerta LE, Meijera HEH. Extending the EGP constitutive model for polymer glasses to multiple relaxation times. *J Mech Phys Solids* 2011;59(10):2191–207.
- [23] Krempl E, Khan F. Rate (time)-dependent deformation behavior: an overview of some properties of metals and solid polymers. *Int J Plasticity* 2003;19(7):1069–95.
- [24] Colak OU. Modeling deformation behavior of polymers with viscoplasticity theory based on overstress. *Int J Plasticity* 2005;21(1):145–60.
- [25] Ghorbel E. A viscoplastic constitutive model for polymeric materials. *Int J Plasticity* 2008;24(11):2032–58.
- [26] Senden DJA, Krop S, van Dommelen JAW, Govaert LE. Rate- and temperature-dependent strain hardening of polycarbonate. *J Polym Sci Part B: Polym Phys* 2012;50(24):1680–93.
- [27] Bouvard JL, Bouvard C, Denton B, Tschopp MA, Horstemeyer MF. Simulation of impact tests on polycarbonate at different strain rates and temperatures. 2011. p. 145–7.
- [28] Richeton J, Ahzi S, Daridon L. Thermodynamic investigation of yield-stress models for amorphous polymers. *Philos Mag* 2007;87(24):3629–43.
- [29] Richeton J, Ahzi S, Daridon L, Rémond Y. Modeling of strain rates and temperature effects on the yield behavior of amorphous polymers. *J de Physique Archives* 2003;110:39–44.
- [30] Richeton J, Ahzi S, Daridon L, Rémond Y. A formulation of the cooperative model for the yield stress of amorphous polymers for a wide range of strain rates and temperatures. *Polymer* 2005;46(16):6035–43.
- [31] Richeton J, Ahzia S, Vecchiob KS, Jiang FC, Adharapurapub RR. Influence of temperature and strain rate on the mechanical behavior of three amorphous polymers: Characterization and modeling of the compressive yield stress. *Int J Solids Struct* 2006;43(7–8):2318–35.
- [32] Richeton J, Ahzia S, Vecchiob KS, Jiang FC, Makradia A. Modeling and validation of the large deformation inelastic response of amorphous polymers over a wide range of temperatures and strain rates. *Int J Solids Struct* 2007;44(24):7938–54.
- [33] Richeton J, Schlatterb G, Vecchioc KS, Rémond Y, Ahzi S. A unified model for stiffness modulus of amorphous polymers across transition temperatures and strain rates. *Polymer* 2005;46(19):8194–201.
- [34] Zhu Guo-wei, de Ma F, Jia Yu-xi, Qu Peng, Guo Yun-li, Sun Xiao-chen. Resin matrix shear band and its special effect on stress concentration of fiber composites. *Chin J Polym Sci (CJPS)* 2014;32(6):703–10.
- [35] Chen W, Zhang B, Forrestal MJ. A split Hopkinson bar technique for low-impedance materials. *Exp Mech* 1999;39(2):81–5.
- [36] Davies EDH, Hunter SC. The dynamic compression testing of solids by the method of the split Hopkinson pressure bar. *J Mech Phys Solids* 1963;11(3):155–79.
- [37] Davies RM. A critical study of the hopkinson pressure bar. *Philosophical Trans R Soc Lond Ser A, Math Phys Sci* 1948;240(821):375–457.
- [38] Gray III GT, Blumenthal WR, Trujillo CP, Carpenter II RW. Influence of temperature and strain rate on the mechanical behavior of Adiprene L-100. *J Phys IV Fr* 1997;07(C3). C3–C523-C523–528.
- [39] Kolsky H. An investigation of the mechanical properties of materials at very high rates of loading. *Proc Phys Soc Sect B* 1949;676–701.
- [40] Trautmann A, Sivior CR, Walley SM, Field JE. Lubrication of polycarbonate at cryogenic temperatures in the split Hopkinson pressure bar. *Int J Impact Eng* 2005;31(5):523–44.
- [41] Sivior CR, Walley SM, Proud WG, Field JE. The high strain rate compressive behaviour of polycarbonate and polyvinylidene difluoride. *Polymer* 2005;46(26):12546–55.
- [42] Li ZH, John L. strain rate effects on the thermomechanical behavior of polymers. *Int J Solids Struct* 2001;38:3549–62.
- [43] Lerch V, Gary G, Hervé P. Thermomechanical properties of polycarbonate under dynamic loading. *J Phys IV Fr* 2003;110:159–64.
- [44] Mahieux CA, Reifsnider KL. Property modeling across transition temperatures in polymers a robust stiffness temperature model. *Polymer* 2001;42:3281–91.
- [45] Mulliken AD, Boyce MC. Low to high strain rate deformation of amorphous polymers. In: Proceedings of the 2004 SEM X international Congress and Exposition on experimental and applied Mechanics, Costa Mesa; 2004. p. 197.
- [46] Jordan JL, Sivior CR, Foley JR, Brown EN. Compressive properties of extruded polytetrafluoroethylene. *Polymer* 2007;48(14):4184–95.
- [47] Furmanski J, Cady CM, Brown EN. Time–temperature equivalence and adiabatic heating at large strains in high density polyethylene and ultrahigh molecular weight polyethylene. *Polymer* 2013;54(1):381–90.